NASA TECHNICAL MEMORANDUM

NASA TM X-73, 176

NASA TM X-73, 176

SIDE FORCES ON A TANGENT OGIVE FOREBODY WITH A FINENESS RATIO OF 2.5 AT HIGH ANGLES OF ATTACK AND LOW SPEED

Earl R. Keener and Jose Valdez

Ames Research Center
Moffett Field, California

December 1976

1. Report No.	2. Government Accession No.	3. Recipient's Catalog No.
NASA TM X-73,176		

4. Title and Subtitle	5. Report Date
SIDE FORCES ON A TANGENT OGIVE FOREBODY WITH A FINENESS RATIO OF 2.5 AT HIGH ANGLES OF ATTACK AND LOW SPEED	December 1976
	6. Performing Organization Code
7. Author(s)	8. Performing Organization Report No.
Earl R. Keener and Jose Valdez	A-6797
	10. Work Unit No.
9. Performing Organization Name and Address	505-06-97
NASA Ames Research Center, Moffett Field, Ca. 94035 and ARO, Inc., Moffett Field, Ca. 94035	11. Contract or Grant No.
	13. Type of Report and Period Covered
12. Sponsoring Agency Name and Address	Technical Memorandum
National Aeronautics and Space Administration Washington, D. C. 20546	14. Sponsoring Agency Code

15. Supplementary Notes

16. Abstract

An experimental investigation was conducted in the Ames 12-Foot Pressure Wind Tunnel to determine the subsonic aerodynamic characteristics, at high angles of attack, of a tangent ogive forebody with a fineness ratio of 2.5. Static longitudinal and lateral-directional stability data were obtained at Reynolds numbers ranging from 0.4×10^6 to 3.7×10^6 (based on base diameter) at a Mach number of 0.25. Angle of attack was varied from 36° to 88° at zero sideslip.

The investigation was particularly concerned with the possibility of large side forces and yawing moments at high angles of attack at zero sideslip. It was found that at low Reynolds numbers the forebody does not have a side force at high angles of attack; however, at Reynolds numbers above about 2×10^6, a side force occurs in the angle-of-attack range from 45° to 80°. The angle of onset of side force of 45°, or higher, agrees with the angle predicted from previous results. The maximum side force is as large as the maximum normal force. The maximum normal force coefficient varies between 1.0 and 2.0 over the Reynolds number range tested and occurs at angles of attack near 65°, rather than at 90°.

17. Key Words (Suggested by Author(s))	18. Distribution Statement
Aerodynamic characteristics Bodies Subsonic High angle of attack Side forces	unlimited STAR Category 02

19. Security Classif. (of this report)	20. Security Classif. (of this page)	21. No. of Pages	22. Price*
Unclassified	Unclassified	24	3.25

*For sale by the National Technical Information Service, Springfield, Virginia 22161

SIDE FORCES ON A TANGENT OGIVE FOREBODY WITH A FINENESS RATIO OF 2.5 AT HIGH ANGLES OF ATTACK AND LOW SPEED

Earl R. Keener and Jose Valdez*

Ames Research Center

SUMMARY

An experimental investigation was conducted in the Ames 12-Foot Pressure Wind Tunnel to determine the subsonic aerodynamic characteristics, at high angles of attack, of a tangent ogive forebody with a fineness ratio of 2.5. Static longitudinal and lateral-directional stability data were obtained at Reynolds numbers ranging from 0.4×10^6 to 3.7×10^6 (based on base diameter) at a Mach number of 0.25. Angle of attack was varied from 36° to 88° at zero sideslip.

The investigation was particularly concerned with the possibility of large side forces and yawing moments at high angles of attack at zero sideslip. It was found that at low Reynolds numbers the forebody does not have a side force at high angles of attack; however, at Reynolds numbers above about 2×10^6, a side force occurs in the angle-of-attack range from 45° to 80°. The angle of onset of side force of 45°, or higher, agrees with the angle predicted from previous results. The maximum side force is as large as the maximum normal force. The maximum normal force coefficient varies between 1.0 and 2.0 over the Reynolds number range tested and occurs at angles of attack near 65°, rather than at 90°.

INTRODUCTION

When a body of revolution is pitched to high angles of attack, a side force can occur at zero sideslip angle. This side force results when the separation-induced vortex flow field on the lee side of the body becomes asymmetric. Since the configuration of the forebody can play an important role in the stability and control characteristics of aircraft and missiles at high angles of attack, a comprehensive wind-tunnel investigation was undertaken at Ames Research Center to obtain static aerodynamic data for forebody-alone and forebody-plus-afterbody models. The tests included a wide range of forebody shapes, afterbody lengths, Reynolds numbers, and Mach numbers. Reports thus far generated from this test program are listed in references 1 to 8.

*Project Engineer, ARO, Inc., Moffett Field, Calif. 94035.

It was found from tests of forebody-alone models with pointed noses and fineness ratios of 3.5 and 5 that large side forces can develop at high angles of attack and zero sideslip at subsonic speeds. The magnitude of the side forces can be larger than the maximum normal force. The angle of attack of onset of side force varies only with forebody geometry and can be correlated with the semiapex angle of the nose by a simple formula: onset $\alpha \simeq 2\delta_N$.

The formula for the angle of attack of onset of side force for pointed forebodies predicts that the angle of attack range in which a side force occurs can be increased beyond the operating range of the aircraft or missile by increasing the nose angle (decreasing the fineness ratio). To further test this prediction of the effect of forebody on the angle of attack of onset of side force, a tangent-ogive forebody with a fineness ratio of 2.5 (semiapex angle of 22.6) was tested at low speed. The predicted angle of attack of onset of side force for this forebody is 45° or higher. The investigation was conducted in the Ames 12-Foot Pressure Wind Tunnel at a Mach number of 0.25 and at Reynolds numbers from 0.4×10^6 to 3.7×10^6 (based on model base diameter) and at angles of attack from 36° to 88°.

NOMENCLATURE

The axis system and sign convention are presented in figure 1. The data are presented in the body axis coordinate system with the moment center located at the base of the forebody model.

ACY	absolute value of C_Y
C_m	pitching-moment coefficient, pitching moment/qSd
$C_{m,R}$	resultant-moment coefficient, $(C_n \sin \Psi + C_m \cos \Psi)$
C_n	yawing-moment coefficient, yawing moment/qSd
C_N	normal-force coefficient, normal force/qS
CP_R	resultant-force center of pressure location, fraction of length ℓ from nose tip, $[1 - (C_{m,R}/C_R)(d/\ell)]$
C_R	resultant-force coefficient in body axis system, $\sqrt{C_N^2 + C_Y^2}$
C_Y	side-force coefficient, side-force/qS

d	base diameter, 15.24 cm
ℓ	length of forebody, 38.1 cm
MACH	free-stream Mach number
q	free-stream dynamic pressure
R	Reynolds number, based on model base diameter, millions
S	area of forebody base
α	angle of attack, deg
BETA	angle of sideslip, deg
δ_N	semiapex angle of the nose (22.6°)
Ψ	$\tan^{-1}(C_Y/C_N)$

Model Configuration Code

AD	ℓ/d = 3.5 afterbody detached from forebody (separated by 0.16 cm gap), but attached to sting
NS FT2.5	tangent-ogive forebody with sharp nose ℓ/d = 2.5

TEST FACILITY

The aerodynamic data presented here were obtained from wind tunnel tests conducted in the Ames 12-Foot Pressure Wind Tunnel. This tunnel is a variable-pressure, low-turbulence facility with a Mach number range from 0.1 to about 0.9 and a unit Reynolds number capability up to about 26×10^6/m at a Mach number of 0.25. Eight fine-mesh screens in the settling chamber, together with a contraction ratio of 25 to 1, provide an airstream of exceptionally low turbulence.

MODEL DESCRIPTION

The forebody model is a tangent ogive with a fineness ratio (ℓ/d) of 2.5 and a base diameter of 15.24 cm. An ℓ/d = 3.5 afterbody was available from previous tests. It could be clamped to the sting but free of the forebody (0.16-cm gap) so that forebody forces could be measured in the presence of the afterbody.

TEST CONDITIONS AND PROCEDURES

The investigation was conducted at Reynolds numbers ranging from 0.4×10^6 to 3.7×10^6 (based on base diameter) at a Mach number of 0.25. The model was mounted from a floor support system that provided a high angle of attack range (fig. 2). Since it was not possible to pitch the model continuously from $\alpha = 0°$ to 88°, the sting support shown in figure 2 was used for the data presented herein for $\alpha = 36°$ to 88°, which was the angle of attack range of principle interest in this investigation. Aerodynamic forces and moments on the model were measured using an internal-six-component strain gage balance. The $\ell/d = 2.5$ tangent-ogive forebody was tested first without the afterbody. A few tests were then made in the presence of the afterbody (afterbody clamped to the sting but free of the forebody) to determine the effect of the flow around the base on the forces and moments.

DATA REDUCTION AND ACCURACY

The six-component force and moment data were reduced about the model moment-reference center in the body axis system. The moment center was located on the model centerline at the base of the forebody. Angle of attack was corrected for deflection of the sting and balance under aerodyramic load. Appropriate aerodynamic coefficients were corrected for model weight tares. Stream angles as large as 2° are known to have existed in the vicinity of the model due to the influence of the support system fairing on the tunnel floor (fig. 2); however, no stream angle corrections were applied to the data. Mean values of the forces and pressures were recorded by electronic filtering and, in addition, three samples of all the balance and tunnel static pressure data were averaged for each data point and then reduced to coefficient form.

Data repeatability for the principle parameters was estimated by reviewing repeat points and is as follows:

α	$= \pm 0.03°$	C_N	$= \pm 0.03$
R	$= \pm 0.02$	C_Y	$= \pm 0.02$
		C_m	$= \pm 0.03$

PRESENTATION OF RESULTS

Table 1 presents an index of the figures in which the data are presented. Figures 3 to 5 present a comparison of the results from the

forebody tested alone with the results of the forebody tested in the presence of the afterbody. Figure 6 presents the results from the forebody tested alone at several Reynolds numbers from 0.4×10^6 to 3.7×10^6. The data are plotted and faired as a function of angle of attack using an automatic data plotting system. The data cover the angle of attack range from 36° to 88°, obtained from the high angle of attack sting support.

DISCUSSION

The primary purpose of this investigation was to determine if a side force develops at zero sideslip for a tangent ogive forebody having a fineness ratio of 2.5.

Comparison of Forebody Alone to Forebody In Presence of Afterbody Results

There was some concern that the data obtained with the forebody alone might not represent adequately the contribution of the forebody to the asymmetric side force and moment on a forebody-afterbody configuration because of possible interference between the flow around the base and the flow over the upper surface. To investigate this effect, tests were made first with the forebody alone mounted on the balance and then with the afterbody attached to the sting but separated slightly from the forebody (forebody forces in the presence of the afterbody). The results are compared in figures 3, 4, and 5 for Reynolds numbers (based on base diameter) of 0.8×10^6, 1.5×10^6 and 2×10^6 at M = 0.25.

At a Reynolds number of 2×10^6 a moderate side force occurs. There is a noticeable difference in the variation of side force with angle of attack as well as a small difference in maximum magnitude for the two configurations. Also, at very high angles of attack of 80° to 88° there is a small side force for the forebody alone, but not in the presence of the afterbody. The angle of attack of onset of side force is the same for both configurations. At all Reynolds numbers (figs. 3 to 5) the normal force is as much as 18 percent lower for the forebody alone than in the presence of the afterbody, which is attributed to the end effect of the base, which reduces the lift generated by the forebody.

Effect of Reynolds Number

The results of tests with the forebody alone at Reynolds numbers from 0.4×10^6 to 3.7×10^6 are presented in figure 6. No side force occurs at a Reynolds number of 0.4×10^6; however, at a Reynolds number of 0.8×10^6 a small side force (maximum $|C_Y| = 0.2$) exists at angles of attack above 60°. As

the Reynolds number increases to 3.7×10^6, the magnitude of the side force increases to maximum $|C_Y|=1.4$. These results are different from those of the $\ell/d = 3.5$ and 5 tangent ogive forebodies (refs. 4 and 5) for which the magnitude of the side forces are a maximum at the lower Reynolds numbers. Note that the angle of attack of onset of side force is 45° to 50°, which agrees with the predicted value of 45° from the simple formula from reference 1: onset $\alpha \simeq 2\delta_N$ ($\delta_N = 22.6°$). The side force exists to an angle of attack of about 80° for the forebody in the presence of the afterbody (fig. 5). From the plot of AC_Y/C_N vs angle of attack, the magnitude of the maximum side force is as large as the normal force at a Reynolds number of 3.7×10^6 at angles of attack of 65° to 70°.

The normal force coefficient has a maximum value of about 2.0 at the lowest Reynolds number of 0.4×10^6, decreases to about 1.0 at a Reynolds number of 1×10^6 and then increases to about 1.4 at a Reynolds number of 3.7×10^6. The maximum C_N occurs at angles of attack between 60° and 70°, rather than at 90°.

CONCLUSIONS

The following conclusions are made from the data obtained from a wind-tunnel investigation to determine the asymmetric forces and moments generated on an $\ell/d = 2.5$ tangent ogive at high angles of attack and at zero sideslip. Data were obtained over a wide range of angles of attack, and Reynolds numbers.

1. At low Reynolds numbers the forebody does not have a side force at high angles of attack; however, at Reynolds numbers above about 2×10^6 (based on base diameter), a side force occurs in the angle-of-attack range from 45° to 80°.

2. The angle of onset of side force of 45° or higher agrees with the angle predicted from previous results.

3. The maximum side force is as large as the maximum normal force.

4. The maximum normal force coefficient varies between 1.0 and 2.0 over the Reynolds number range tested and occurs at angles of attack near 65°, rather than at 90°.

Ames Research Center
National Aeronautics and Space Administration
Moffett Field, California

November 15, 1976

REFERENCES

1. Keener, Earl R.; and Chapman, Gary T.: Onset of Aerodynamic Side Forces at Zero Sideslip on Symmetric Forebodies at High Angles of Attack. AIAA Paper 74-770, Aug. 1974.

2. Keener, Earl R.; and Taleghani, Jamshid: Wind Tunnel Investigation of the Aerodynamic Characteristics of Five Forebody Models at High Angles of Attack at Mach Numbers From 0.25 to 2. NASA TM X-73,076, 1975.

3. Keener, E. R.; Chapman, G. T.; and Kruse, R. L.: Effects of Mach Number and Afterbody Length on Onset of Asymmetric Forces on Bodies at Zero Sideslip and High Angles of Attack. AIAA Paper 76-66, Jan. 1976.

4. Keener, Earl R.; Chapman, Gary T.; Cohen, Lee; and Taleghani, Jamshid: Side Forces on a Tangent Ogive Forebody With a Fineness Ratio of 3.5 at High Angles of Attack and Mach Numbers from 0.1 to 0.7. NASA TM X-3437, 1976.

5. Keener, Earl R.; Chapman, Gary T.; Cohen, Lee; and Taleghani, Jamshid: Side Forces on Forebodies at High Angles of Attack and Mach Numbers From 0.1 to 0.7: Two Tangent Ogives, Paraboloid and Cone. NASA TM X-3438, 1976.

6. Jorgensen, Leland H.; and Nelson, Edgar R.: Experimental Aerodynamic Characteristics for a Cylindrical Body of Revolution with Various Noses at Angles of Attack from 0 to 58° and Mach Numbers from 0.6 to 2.0. NASA TM X-3128, 1974.

7. Jorgensen, Leland H.; and Nelson, Edgar R.: Experimental Aerodynamic Characteristics for Bodies of Elliptic Cross Section at Angles of Attack From 0 to 58° and Mach Numbers From 0.6 to 2.0. NASA TM X-3129, 1975.

8. Jorgensen, Leland H.; and Nelson, Edgar R.: Experimental Aerodynamic Characteristics for a Cylindrical Body of Revolution With Side Strakes and Various Noses at Angles of Attack From 0 to 58° and Mach Numbers From 0.6 to 2.0. NASA TM X-3130, 1975.

TABLE 1. - INDEX OF DATA FIGURES

Notes:

1. Positive directions of force coefficients, moment coefficients, and angles are indicated by arrows
2. For clarity, origins of wind and stability axes have been displaced from the center of gravity

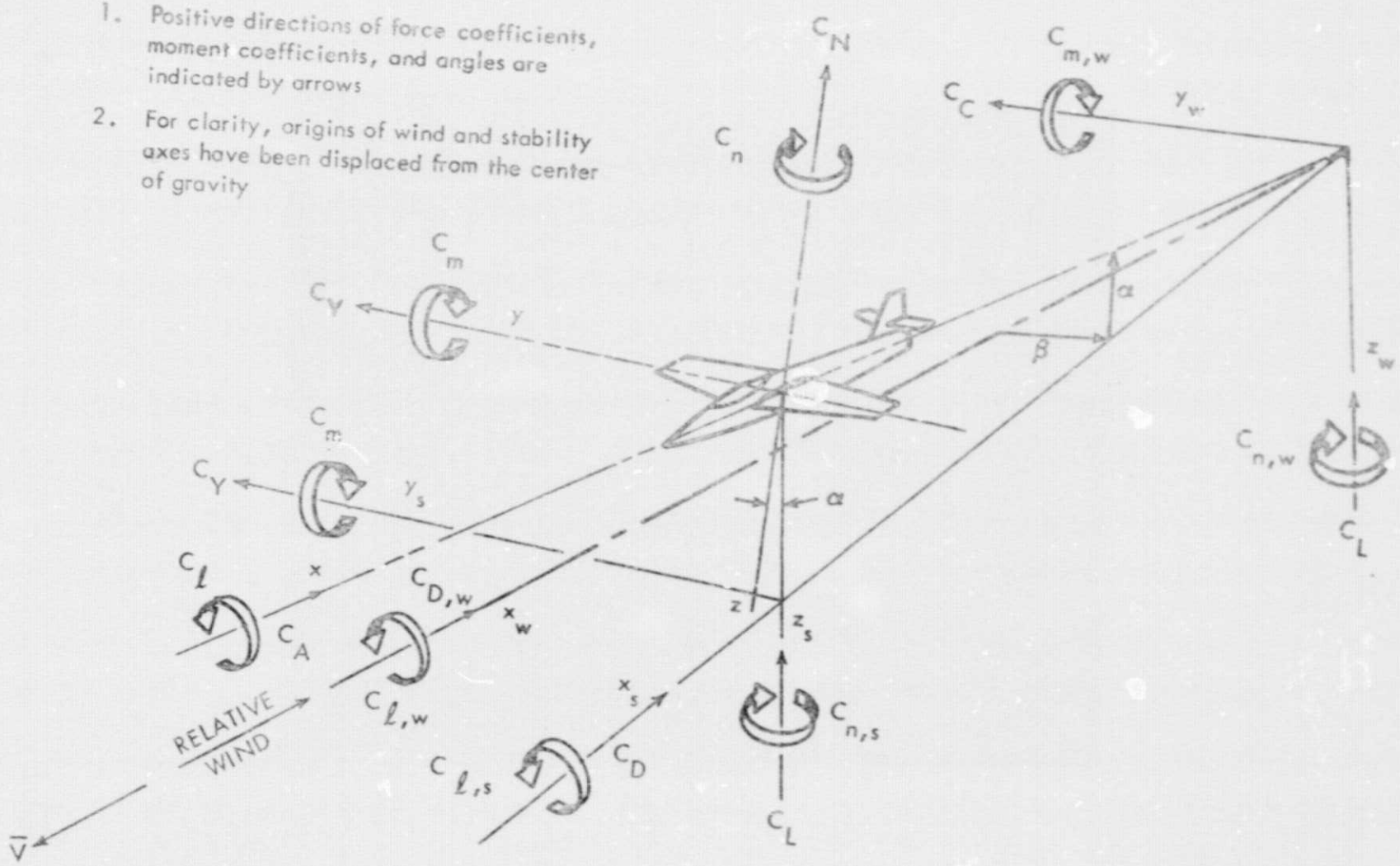

Figure 1. Axis systems, showing direction and sense of force and moment coefficients, angle of attack, and sideslip angle.

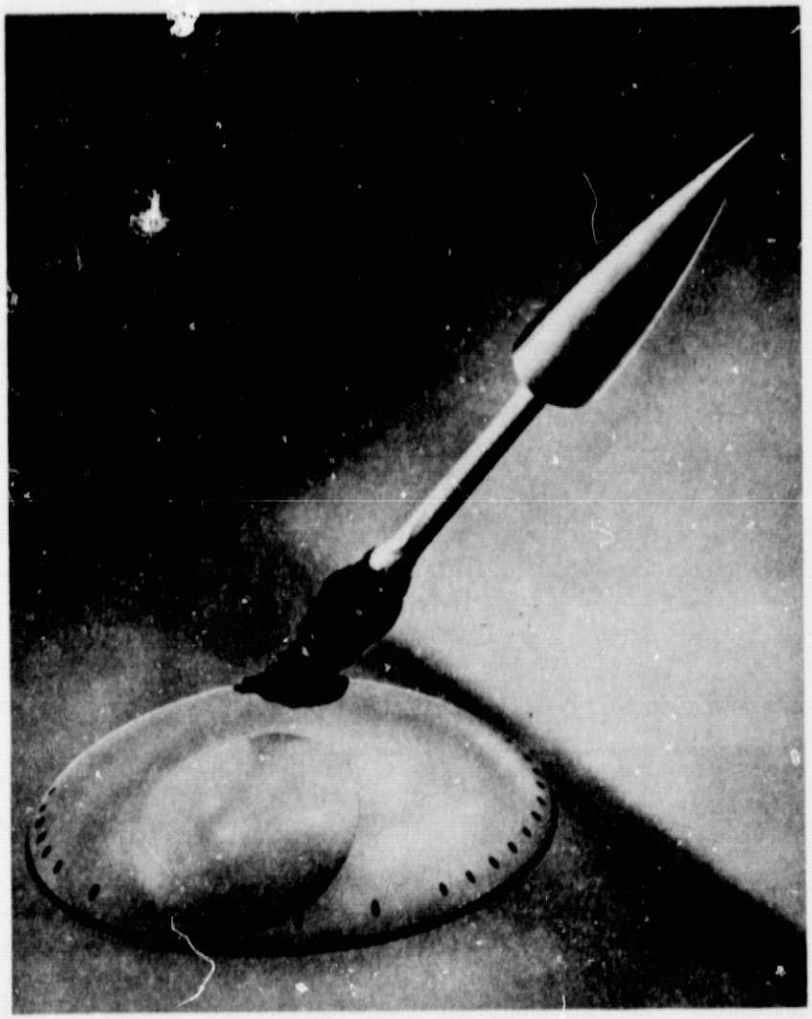

Figure 2. - Photograph of model support set-up for α = 36° to 88°.

DATA

DATA SET	SYMBOL	CONFIGURATION	BETA	MACH
BHI109	○	NS FT2.5	.000	.250
BHI145	□	NS FT2.5 AD	.000	.250

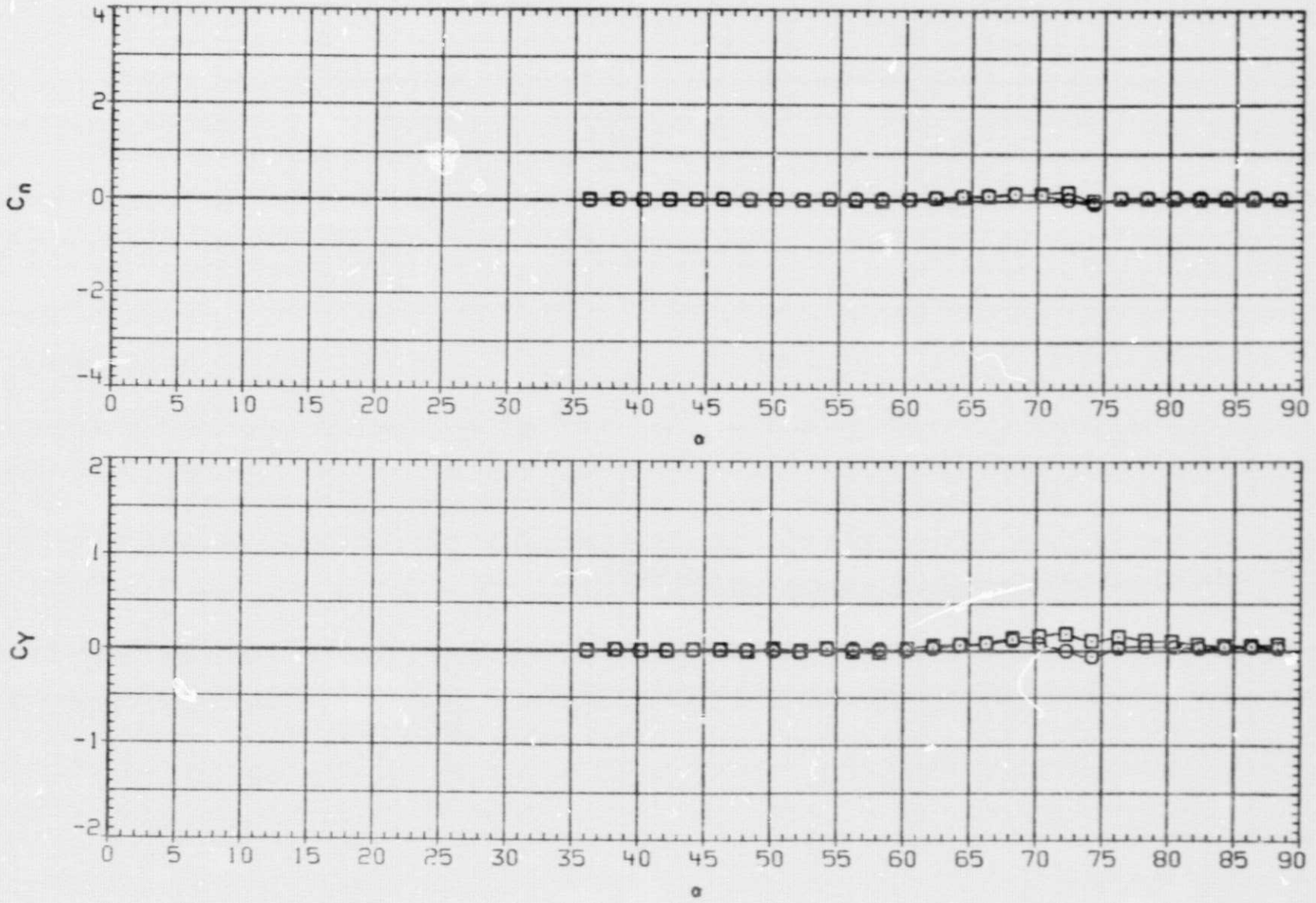

FIG.3 COMPARISON OF FOREBODY-ALONE TO FOREBODY-IN-PRESENCE-OF-AFTERBODY RESULTS, REY. NO. = 0.8 MILLION

(A)R = .80

DATA SET SYMBOL CONFIGURATION

BH1109	○	NS FT2.5
BH1145	□	NS FT2.5 AD

BETA	MACH
.000	.250
.000	.250

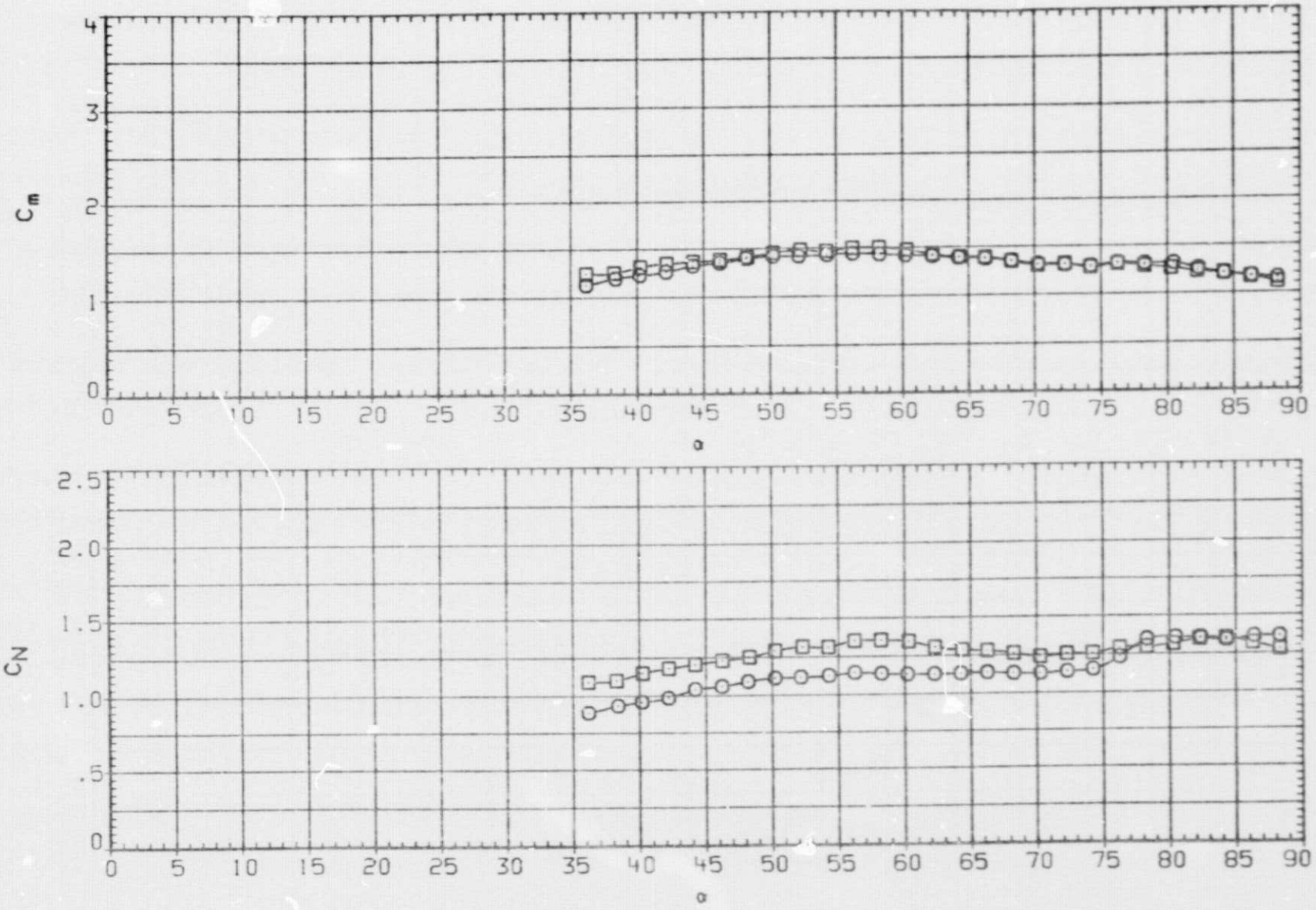

FIG.3 COMPARISON OF FOREBODY-ALONE TO FOREBODY-IN-PRESENCE-OF-AFTERBODY RESULTS, REY. NO. = 0.8 MILLION

(A)R = .80

DATA SET	SYMBOL	CONFIGURATION	BETA	MACH
BH1107	○	NS FT2.5	.000	.250
BH1145	□	NS FT2.5 AD	.000	.250

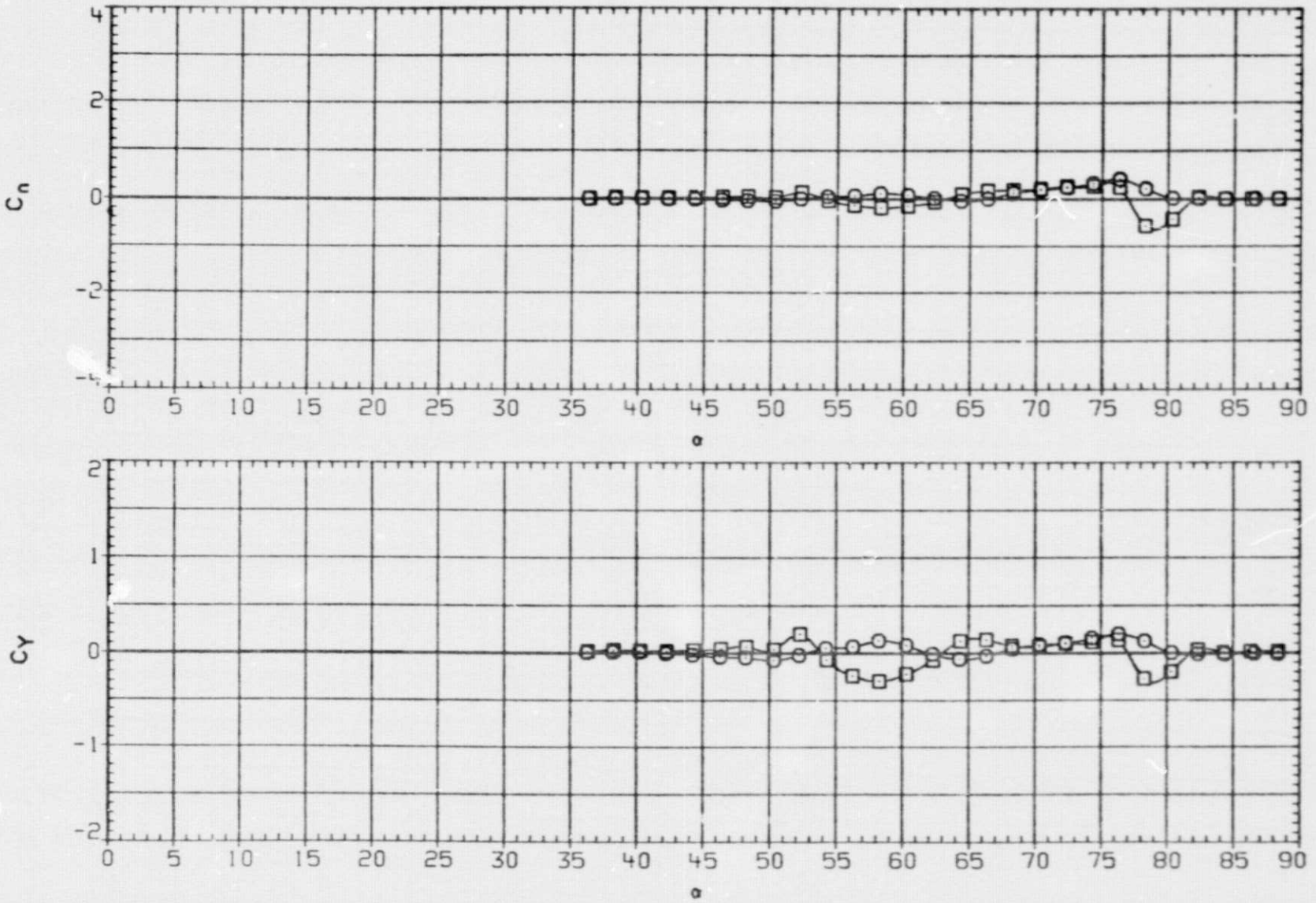

FIG.4 COMPARISON OF FOREBODY-ALONE TO FOREBODY-IN-PRESENCE-OF-AFTERBODY RESULTS, REY. NO. = 1.5 MILLION

(A)R = 1.50

DATA SET	SYMBOL	CONFIGURATION	BETA	MACH
BH1107	○	NS FT2.5	.000	.250
BH1145	□	NS FT2.5 AD	.000	.250

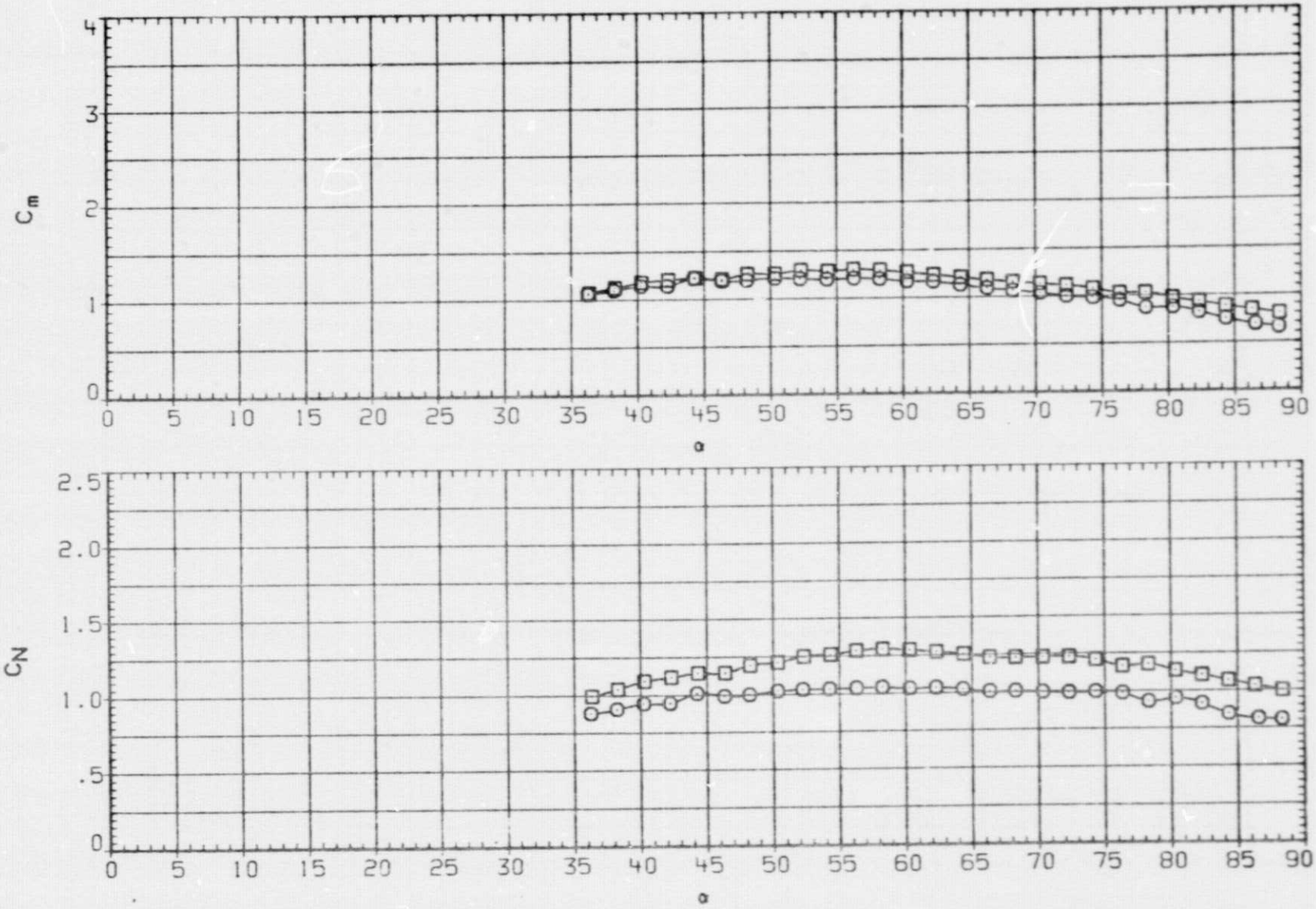

FIG.4 COMPARISON OF FOREBODY-ALONE TO FOREBODY-IN-PRESENCE-OF-AFTERBODY RESULTS. REY. NO. = 1.5 MILLION

(A)R = 1.50

DATA SET	SYMBOL	CONFIGURATION	BETA	MACH
BH1107	○	NS FT2.5	.000	.250
BH1145	□	NS FT2.5 AD	.000	.250

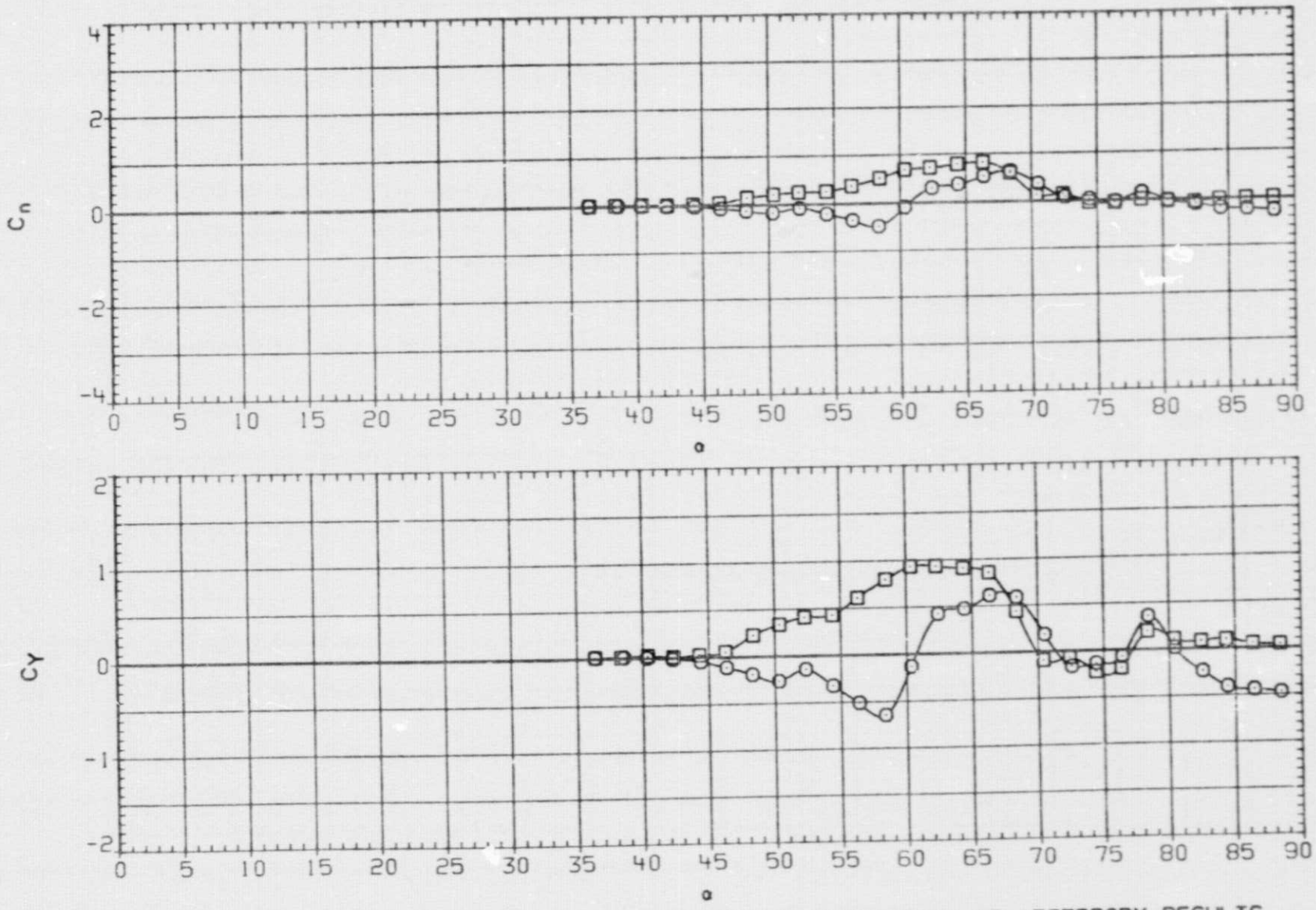

FIG.5 COMPARISON OF FOREBODY-ALONE TO FOREBODY-IN-PRESENCE-OF-AFTERBODY RESULTS, REY. NO. = 2.0 MILLION

(A)R = 2.00

DATA SET	SYMBOL	CONFIGURATION	BETA	MACH
BH1107	○	NS FT2.5	.000	.250
BH1145	□	NS FT2.5 AD	.000	.250

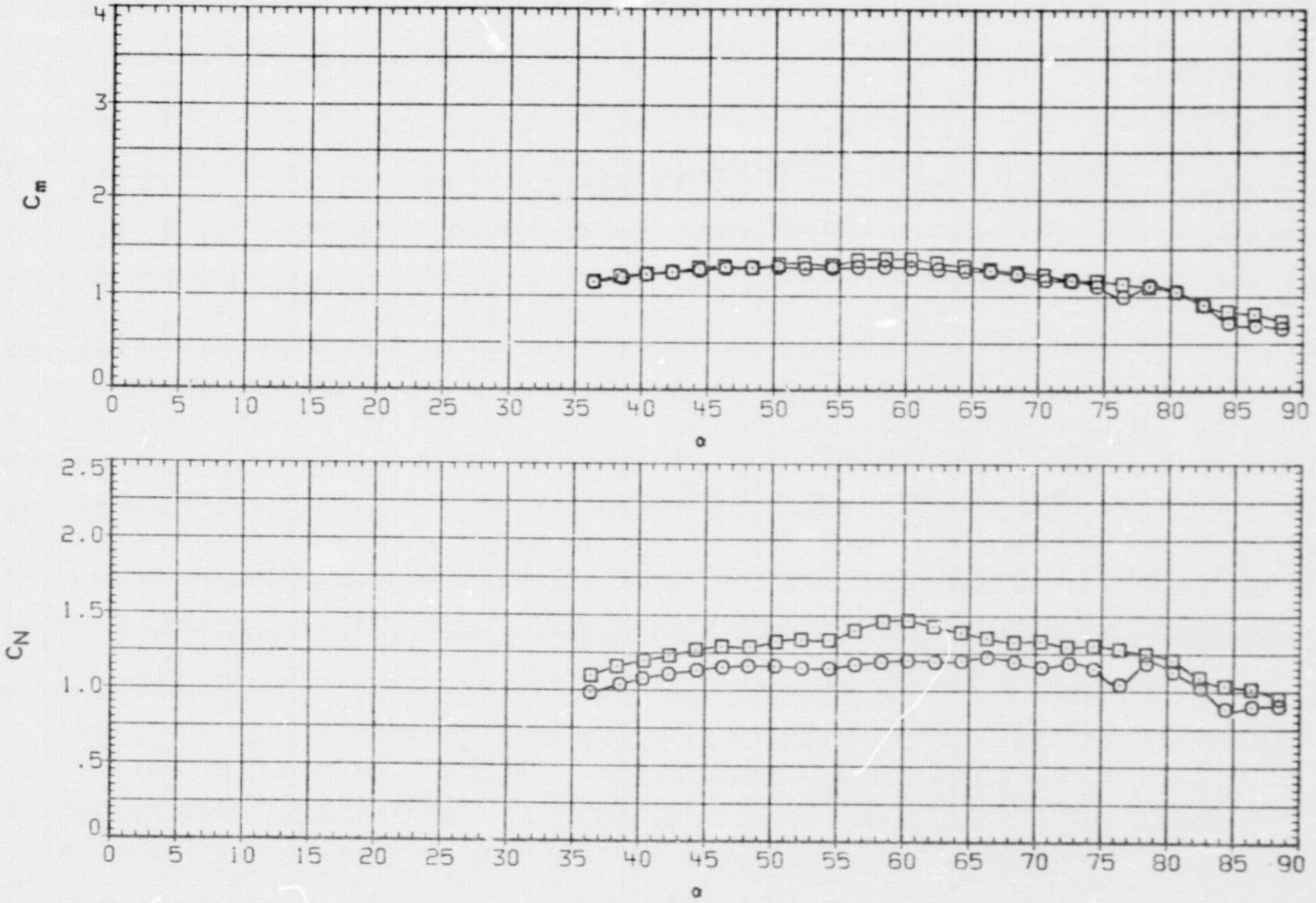

FIG.5 COMPARISON OF FOREBODY-ALONE TO FOREBODY-IN-PRESENCE-OF-AFTERBODY RESULTS, REY. NO. = 2.0 MILLION

(A)R = 2.00

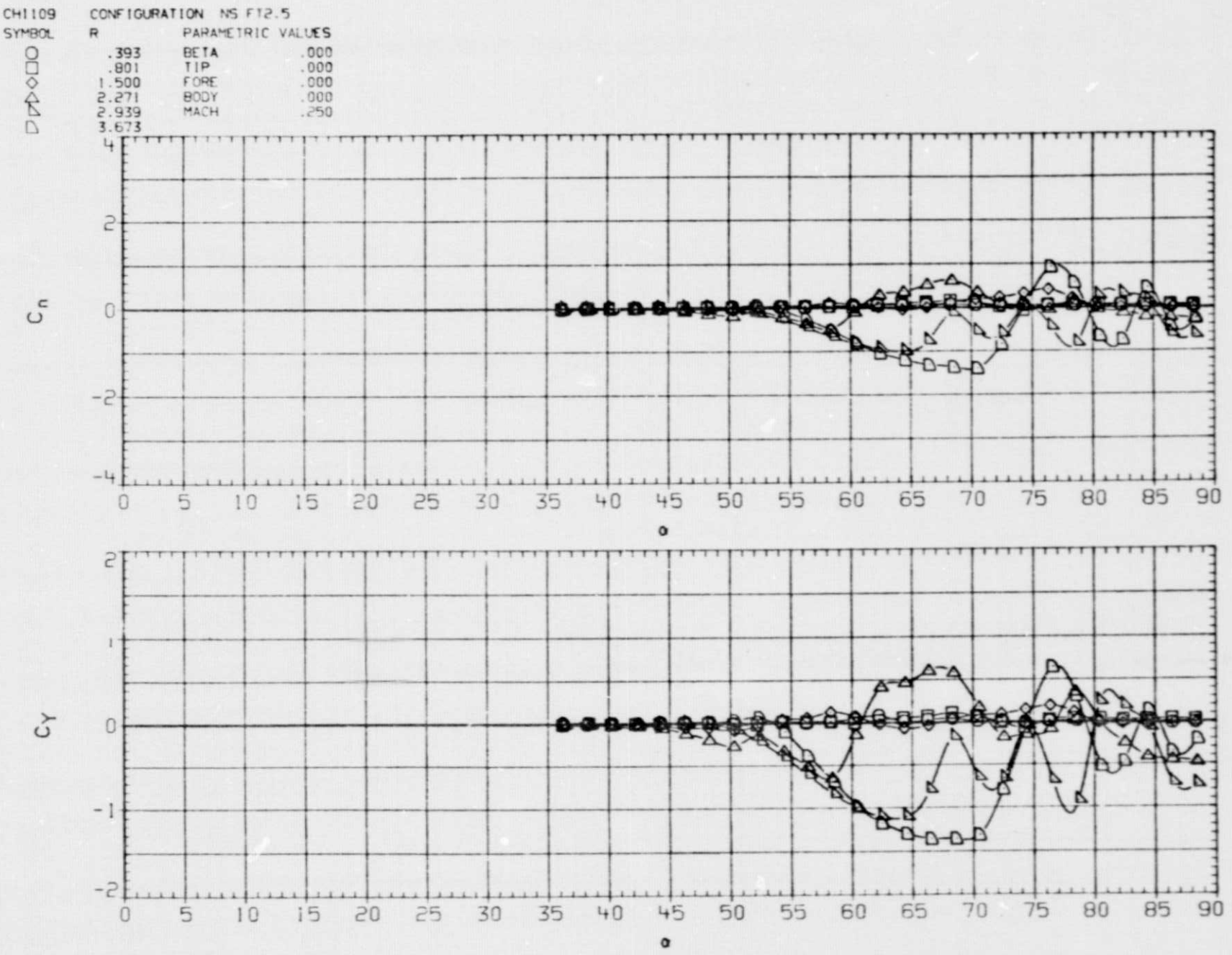

FIG.6 EFFECT OF REYNOLDS NUMBER ON AERODYNAMIC CHARACTERISTICS OF FOREBODY-ALONE MODEL

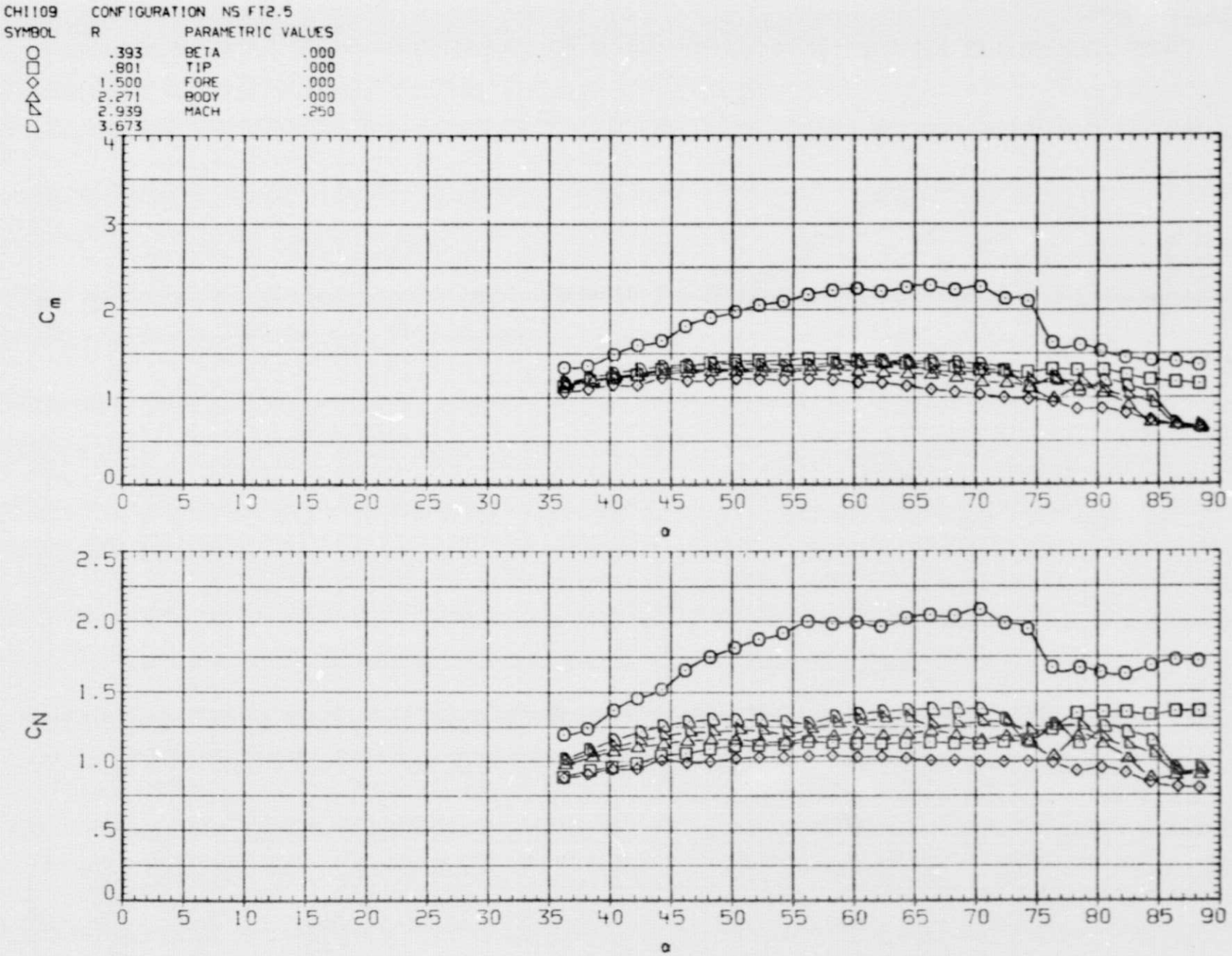

FIG.6 EFFECT OF REYNOLDS NUMBER ON AERODYNAMIC CHARACTERISTICS OF FOREBODY-ALONE MODEL

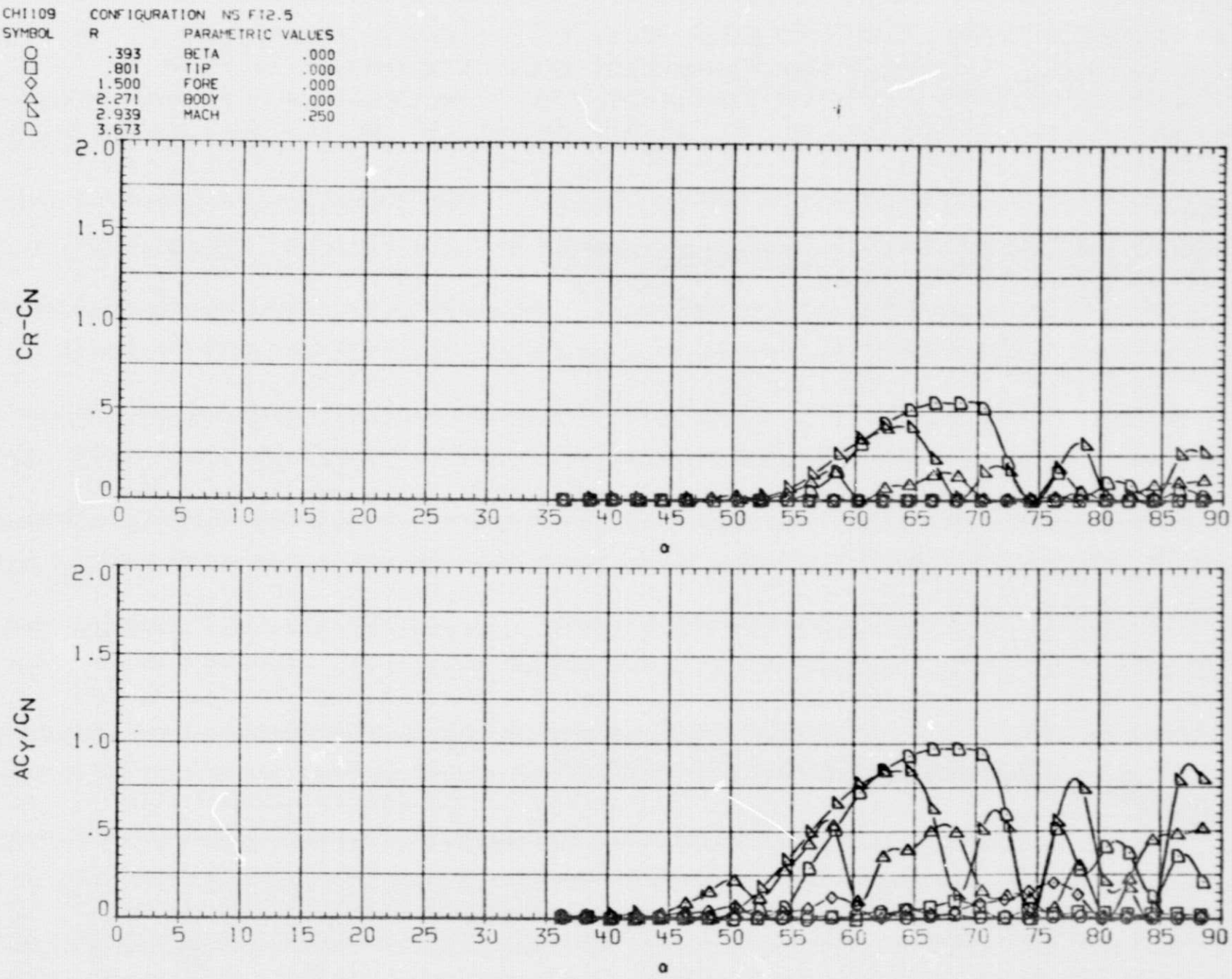

FIG.6 EFFECT OF REYNOLDS NUMBER ON AERODYNAMIC CHARACTERISTICS OF FOREBODY-ALONE MODEL

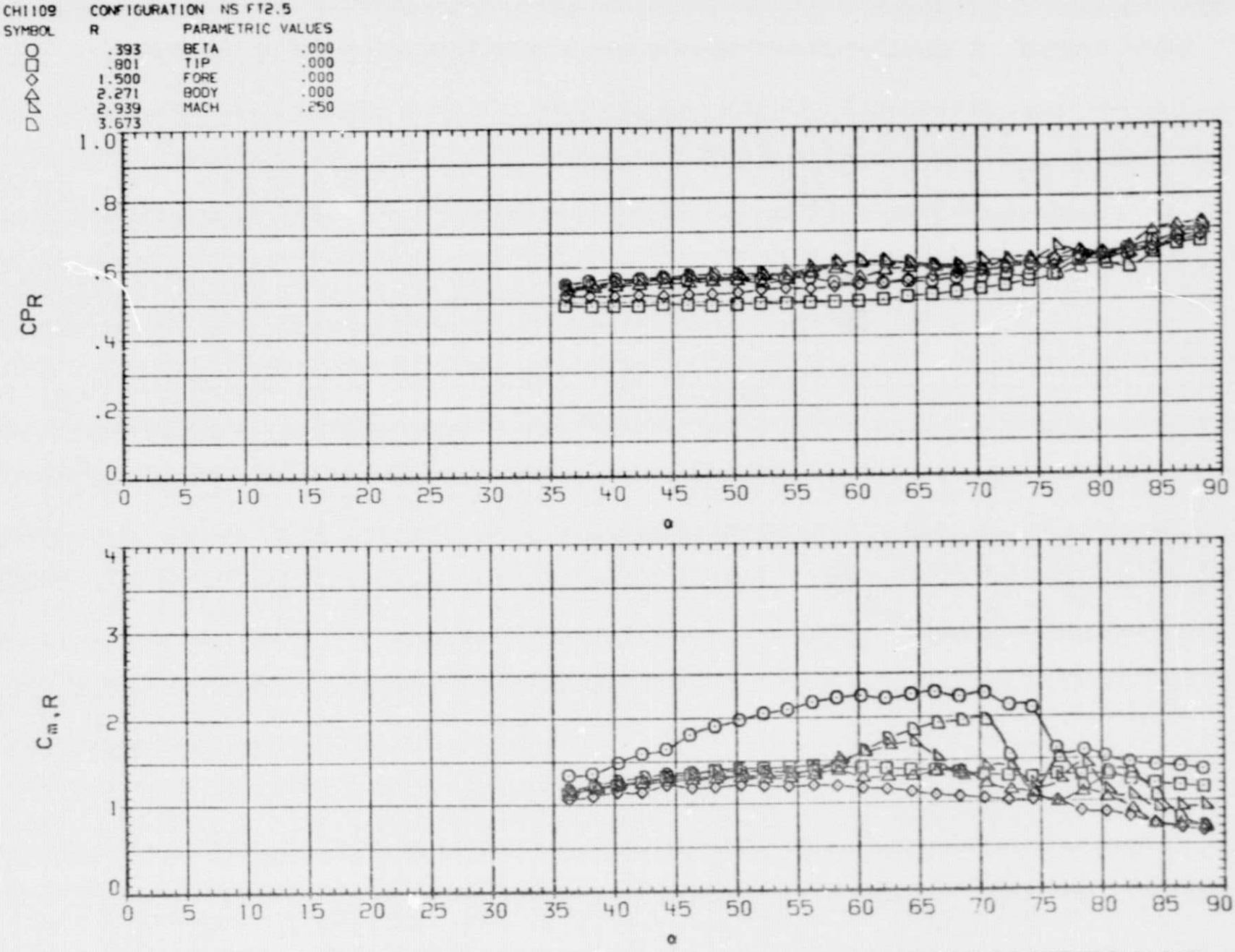

FIG.6 EFFECT OF REYNOLDS NUMBER ON AERODYNAMIC CHARACTERISTICS OF FOREBODY-ALONE MODEL